

## Morphological, elemental and diffused phase transition of La modified PbTiO<sub>3</sub> Ceramics

Niranjan Sahu

P.G. Department of Physics,  
G.M. University,  
Sambalpur-768004, Odisha, India.

### Abstract

The Pb<sub>1-x</sub>La<sub>x</sub>TiO<sub>3</sub> (for x=0.0, 0.10, 0.25, 0.30 and 0.50) compounds were prepared by conventional solid state route. The X-ray diffraction (XRD) pattern was recorded at room temperature and the samples were found in single phase form. The microstructural analysis of the surface of the ceramic compound by scanning electron microscopy (SEM) exhibits that there is a significant change in grain size. It is found that the grain size increases with increase of La concentration. The energy dispersive X-ray spectroscopy (EDS) analysis reveals that the materials are uniform and their composition is as per the chemical formulae. It suggests that the material goes transition from ferroelectric to paraelectric phase with the temperature. This is the behavior of a normal ferroelectric material. It is observed that, the T<sub>c</sub> and maximum dielectric constant (ε<sub>m</sub>) decrease with the La concentration. It could be due to the diffusion of dielectric with the La concentration. The remnance ratio (P<sub>r</sub>/P<sub>s</sub>) was found to decrease with increase of La concentration. The high remnant polarization samples can be used as memory application in electronic industry.

**Keywords:** Ceramics; solid state; SEM; EDS; dielectric; Polarization.

**PACS NO:** 77.80.-e, 72.80Tm; 75.40.Cx, 87.63.pn

### 1. Introduction

The mineral perovskite is CaTiO<sub>3</sub> and is actually orthorhombic at room temperature, becoming cubic at temperatures above 900°C [1]. Lead titanate (PbTiO<sub>3</sub>), which exhibits Perovskites structure and a very high Curie temperature T<sub>c</sub> = 490°C, belongs to the most important ferroelectric and piezoelectric families [2]. The perovskite structure has been one of the most versatile structures for tailoring the properties of materials [3, 4]. The Pb-based ceramic oxides have been widely studied due to their excellent ferroelectric, dielectric, and piezoelectric properties [1-3]. Inparticular,PbTiO<sub>3</sub>-based solid solutions have dominated for decades the technological field responsible for the development of piezoelectric materials [4]. The perovskite structure forms the basis of several complex structures, which may be due to intergrowths, oxygen deficiency or due to cation ordering [4, 5]. It has been shown that modification using aluminium, which occupies the B-sites, provides new structural defects, i.e. oxygen vacancies, during the sintering process [6]. Lead oxide also forms a liquid phase above its melting point (890°C), which improves densification, but it also may affect the stoichiometry of the composition, due to its high volatility at the sintering temperatures. Therefore, an excess PbO is usually added to the initial raw materials, in order to prevent the deviation from the stoichiometry by lead loss and also to improve the densification. Lead titanate PbTiO<sub>3</sub> (PT) and lead lanthanum titanate Pb<sub>1-x</sub>La<sub>x</sub>TiO<sub>3</sub> (PLT) are important perovskite ferroelectric materials which show remarkable ferroelectricity, piezoelectricity and pyroelectricity, because of their potential applications in the field of microelectronics and optoelectronics. Lead titanate (PbTiO<sub>3</sub>) has the perovskite (ABO<sub>3</sub>) structure with the Pb atoms occupying the cell corners, Ti occupying the body center, and the oxygen atoms sitting at the face centers[7,8]. The isomorphic substitution of lead with lanthanum gives rise to a decrease in the tetragonality [9]. The PT undergoes a phase transition at a temperature of 490°C from tetragonal (*P4mm*) ferroelectric phase to centrosymmetric cubic (*Pm3m*) paraelectric phase [10-15]. An appropriate incorporation of La into lead titanate tunes the phase transition temperature and consequently makes the PLT material suitable for a wide

range of device applications at room temperature. G. Shirane, *et al* [16] observed that in La modified PT ceramics for temperatures higher than  $T_c$ , a residual short-range structural disorder has been found, which is not to be compatible with the centrosymmetric cubic structure usually observed in the paraelectric phase. It has been suggested that the lanthanum-induced modification concerning  $PbTiO_3$  results in structural changes that can be directly related to the nature of the phase transition [17-19].

## **2. Materials and Method**

The  $Pb_{1-x}La_xTiO_3$  (for  $x=0.0, 0.10, 0.25, 0.30$  and  $0.50$ ) compounds were prepared by conventional solid state route. The stoichiometric ratio of starting compounds such as Lead Oxide ( $PbO$ , 99%), Lanthanum Oxide ( $La_2O_3$ , 99.9%) and Titanium Oxide ( $TiO_2$ , 99%) were weighed by using a high precision electronic balance. The above compounds were mixed and grinded under acetone using agate mortar and pestle. The grinding was carried out under acetone till the acetone evaporates from the mortar. The mixture was ball milled for 8 h for homogeneous mixture and calcined at  $900^\circ C$  for 6h and for phase conformation XRD was taken. The fine powders of the above compound were pressed into cylindrical pellets of 6 mm diameter and 1 mm thickness under a uni-axial pressure of 6 ton using a hydraulic press. Finally the pellets were sintered at  $1100^\circ C$  for over 4h with 5% extra lead oxide to compensate the lead loss at high temperature and then cooled to room temperature at the rate of  $2^\circ C \text{ min}^{-1}$ . All the above sintering processes were carried out in the air. The XRD patterns of all the samples were recorded by using Philips PANalytical X'pert-MPD X-ray diffractometer (XRD) (Model- PW3020) in the department of ceramic engineering, NIT, Rourkela. The  $CuK\alpha$  radiation was used as an X-ray source. The machine was operated at 35KV and 30mA. The data were collected with step size of 0.020 and time constant of 1 second.

## **3. Results and discussion**

### **3.1 Microstructural and compositional analysis**

The scanning electron micrographs were recorded using a JEOL Scanning electron microscope (SEM) (JEOL T-330) at room temperature. SEM photographs of the undoped and La modified samples sintered at  $1100^\circ C$  are shown in the Fig. 1 (a-e). It is observed that the samples are uniform and the grains are in the order of micrometers. The average grain sizes are found to be 1 to  $4.5\mu m$ . It is found that the grain size increases with increase of La concentration.

The compositional analysis was carried out by SEM-Energy dispersive spectroscopy (EDS). The Energy dispersive x-ray spectroscopy (EDS) is shown in the Fig. 2 (a-e) for the samples  $x = 0.0, 0.10, 0.25, 0.30$  and  $0.50$  respectively. The EDS analysis reveals that, all the compositions are as per the prepared sample. The experimental and theoretical EDS values are compared in Table 1. We have observed that, both values are close to each other.

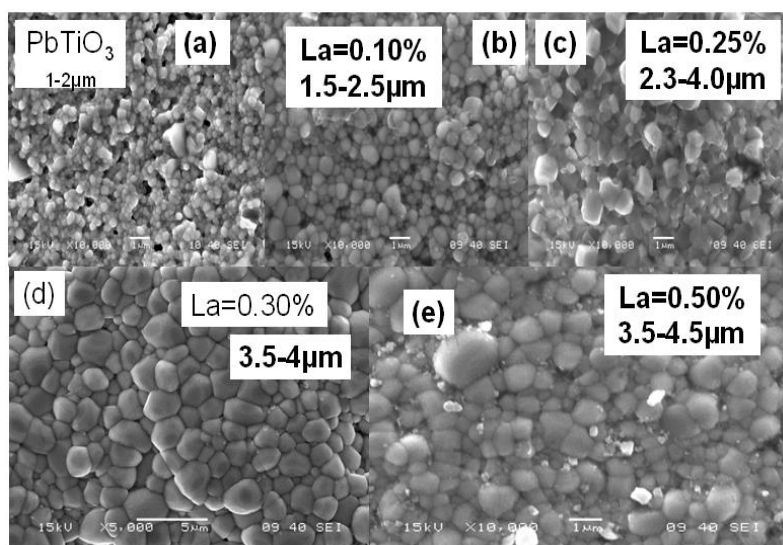


**Fig.1 (a-e):** SEM micrographs of sintered  $Pb_{1-x}La_xTiO_3$  ceramic with (a)  $x=0.00$  (b)  $x=0.10$  (c)  $x=0.25$  (d)  $x=0.30$  and (e)  $x=0.50$ .

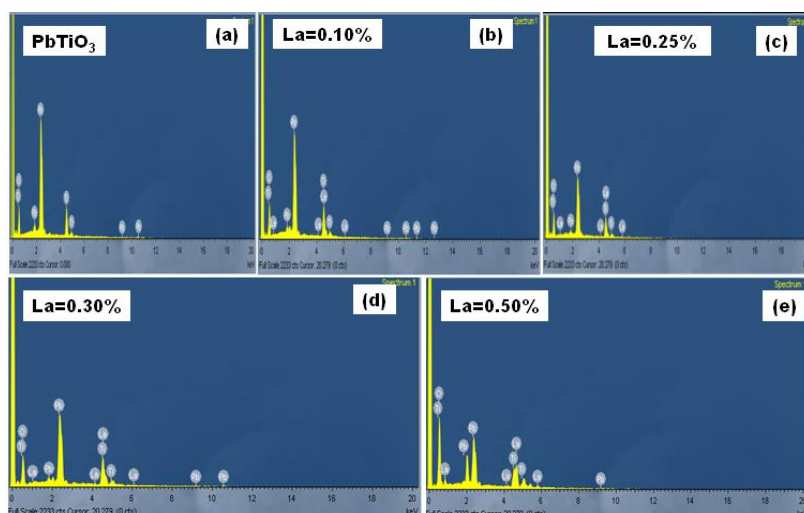


**Fig.2 (a-e):** EDS micrographs of sintered  $Pb_{1-x}La_xTiO_3$  ceramic with (a)  $x = 0.00$ , (b)  $x = 0.10$ , (c)  $x = 0.25$ , (d)  $x = 0.30$ , and (e)  $x = 0.50$ .

**Table 1:** Elemental analysis of pure and La modified PT annealed at 1100°C for 4h.

Composition	Element	Wt % Calculated	Wt% from EDS
Pb <sub>1-x</sub> La <sub>x</sub> TiO <sub>3</sub> x=0.00	Pb	63.60	62.65
	La	0.0	0.0
	Ti	22.77	24.01
	O	13.62	14.34
Pb <sub>1-x</sub> La <sub>x</sub> TiO <sub>3</sub> X=0.10	Pb	53.99	53.05
	La	11.63	11.85
	Ti	21.47	22.45
	O	12.90	12.65
Pb <sub>1-x</sub> La <sub>x</sub> TiO <sub>3</sub> X=0.25	Pb	48.99	48.05
	La	20.63	20.85
	Ti	21.47	22.45
	O	8.90	8.65
Pb <sub>1-x</sub> La <sub>x</sub> TiO <sub>3</sub> x=0.30	Pb	41.48	42.06
	La	26.82	25.35
	Ti	19.79	20.74
	O	14.90	11.05
Pb <sub>1-x</sub> La <sub>x</sub> TiO <sub>3</sub> X=0.50	Pb	34.17	35.73
	La	30.69	30.98
	Ti	18.82	18.98
	O	17.31	14.37

### 3.2 Dielectric Analysis

Temperature variation of dielectric constants ( $\epsilon_r$ ) at different frequencies are shown in the Fig. 3 (a-e) for the samples  $x = 0.00, 0.10, 0.25, 0.30$  and  $0.50$  sintered at  $1100^\circ\text{C}$  for 4h respectively. It is observed that the dielectric constant increases with the temperature and reach to a maximum value and, then decreases with the temperature. It suggests that the material goes transition from ferroelectric to paraelectric phase with the temperature. This is the behavior of a normal ferroelectric material. The temperature at which dielectric constant is maximum has been

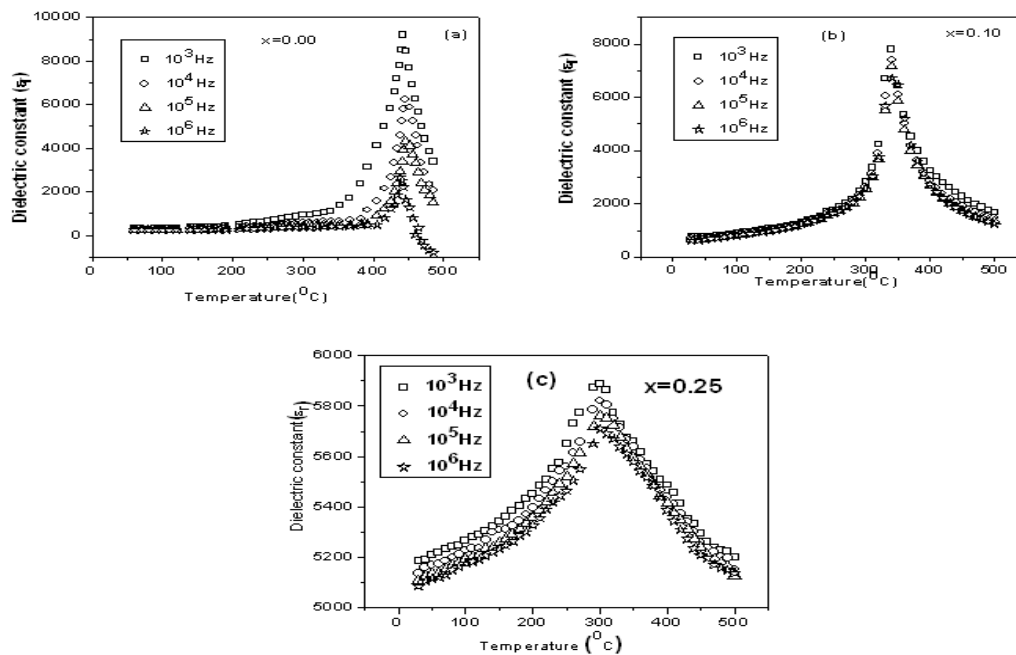
denoted as  $T_c$ . The  $T_c$  was calculated from the temperature versus  $\left| \frac{d\epsilon_r}{dT} \right|$  plot and it was taken

the temperature at  $\left| \frac{d\epsilon_r}{dT} \right|$  is zero. The maximum  $\epsilon_m$  and  $T_c$  values are given in Table 2. It is observed that, the maximum dielectric constant decreases with the frequency. The higher value of  $\epsilon_r$  of low frequency suggests that, the contribution comes from a different type of polarizations i.e. space charge, ionic, electronic etc. However at high frequency the contribution does not come from the polarization having large relaxation time. Mostly the large relaxation time is observed due to space charge polarization. The similar behavior of dielectric response to frequency is observed in other ferroelectric materials [20-23]. The space charge polarization arises from the charge accumulation at grain boundaries and at electrode interfaces. It is mainly due to lead and mobile oxygen vacancies [24].

Again from the Fig.3 (a-e), it is observed that, the  $T_c$  and maximum dielectric constant ( $\epsilon_m$ ) decrease with the La concentration. It could be due to the diffusion of dielectric with the La concentration. The maximum dielectric constant ( $\epsilon_m$ ) decreases with the increase of frequency, which is characteristic of a relaxation phenomenon [25]. For lead titanate type materials, the stability of long range interaction is believed to be suppressed by decoupling effects caused by the

incorporation of ions at the A site of the perovskite structure. Similar behavior has been observed in La doped samples [19-21]. We have calculated the Full Width Half Maximum (FWHM) at the transition temperature from the dielectric constant versus temperature curve. The values are found to be 76.43, 118.12, 153.42, 194.84 and 224.45 for  $x = 0.0, 0.10, 0.25, 0.30$  and  $0.50$  samples respectively. Hence the sample  $x = 0.00, 0.10$  behaves like a normal ferroelectric material. However the large FWHM suggests the samples  $x = 0.25, 0.30$  and  $0.50$  are diffused type ferroelectric material. Also from the Fig. 3 (a-e), depending on the La content, the first case, for temperatures higher than  $T_c$ , a centrosymmetric cubic structure  $Pm\bar{3}m$  is expected since the material undergoes a phase transition to a paraelectric material. In the second case, for temperatures lower than  $T_c$ , a residual short-range structural disorder has been found [26,27] not to be compatible with the centrosymmetric cubic structure usually observed in the ferroelectric phase. At  $x \sim 0.30$ , the dielectric constant shows the similar behavior with the frequency in both paraelectric and ferroelectric regions. Hence, we have taken PLT30 as a parent material in which we have doped transition elements in B site (Ti site) to study the electrical behavior and it has been discussed in my next paper.

The temperature variation of dielectric loss ( $\tan \delta$ ) is shown in Fig.4 (a-e) for the samples  $x = 0.00, 0.10, 0.25, 0.30$  and  $0.50$  respectively at different frequencies (1kHz-1MHz). It has been observed that, the dielectric loss almost constant below  $T_c$  and it increases when approach to  $T_m$ . It is found that dielectric loss decreases with increase of La concentration. It could be due to increase of space charge polarization [21].



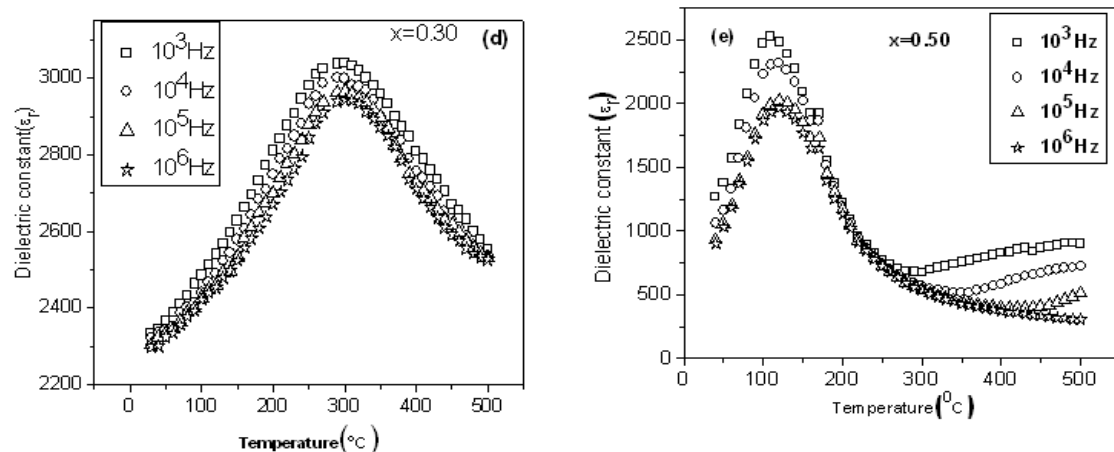


**Fig. 3 (a-e):** The dielectric constants versus temperature of  $Pb_{1-x}La_xTiO_3$ , (a)  $x = 0.0$ , (b)  $x = 0.10$ , (c)  $x = 0.25$ , (d)  $x = 0.30$  and (e)  $x = 0.50$ .

**Table 2:** The observed  $T_c$  and  $\Sigma_m$  obtained from dielectric measurements at different frequencies of  $Pb_{1-x}La_xTiO_3$ ,  $x = 0.0, 0.10, 0.25, 0.30$  and  $0.50$ .

Composition	Frequency (Hz)	$T_c$	$\Sigma_m$
$x = 0.00$	$10^3$	445	9193
	$10^4$	445	6290
	$10^5$	445	4475
	$10^6$	445	2764
$x = 0.10$	$10^3$	340	7790
	$10^4$	340	7402
	$10^5$	340	7151
	$10^6$	340	6724
$x = 0.25$	$10^3$	301	5883
	$10^4$	301	5824
	$10^5$	301	5764
	$10^6$	301	5715
$x = 0.30$	$10^3$	293	3045
	$10^4$	295	3010
	$10^5$	297	2971
	$10^6$	299	2944
$x = 0.50$	$10^3$	110	2527
	$10^4$	113	2339
	$10^5$	116	2042
	$10^6$	118	1954

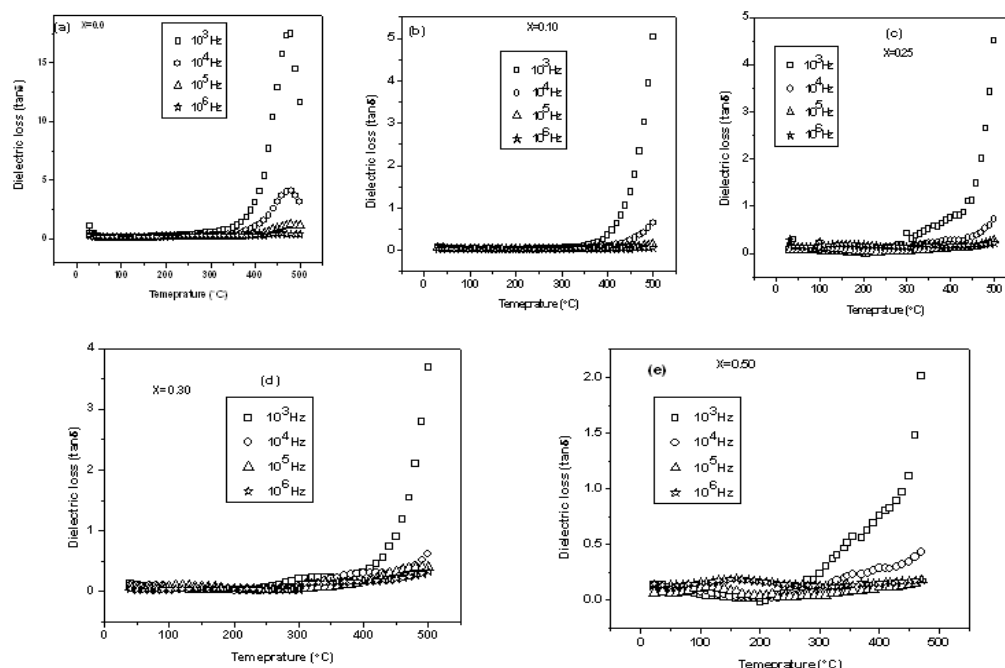


**Fig. 4 (a-e):** The dielectric loss versus temperature of  $Pb_{1-x}La_xTiO_3$ , (a)  $x = 0.0$ , (b)  $x = 0.10$ , (c)  $x = 0.25$ , (d)  $x = 0.30$  and (e)  $x = 0.50$ .

### 3.3 Polarization Study

P-E hysteresis loop is shown in Fig.5 (a-e) for all the samples. All the compositions of the sintered sample at room temperature showed well defined ferroelectric behaviour. The coercive field ( $E_c$ ), remnant polarization ( $P_r$ ), saturation polarization ( $P_s$ ) and remnant ratio ( $P_r/P_s$ ) determined from the hysteresis loops are listed in Table 3.  $P_r$  was found to increase with La concentration from which one can predict that material gets ferroelectrically soften. Domain switching becomes easier because  $La^{3+}$  ions substitutes  $Pb^{2+}$  ions at A site and the presence of multiple ions ( $Pb^{2+}$  and  $La^{3+}$ ) resulted in higher multi-domain polarization as evidenced by increase in  $P_r$  and  $P_s$ . The remnant ratio ( $P_r/P_s$ ) was found to decrease with increase of La concentration. The  $P_r$  and  $E_c$  values are comparable to that reported in the literature for the polycrystalline materials [18, 22]. The high remnant polarization samples can be used as memory application in electronic industry.

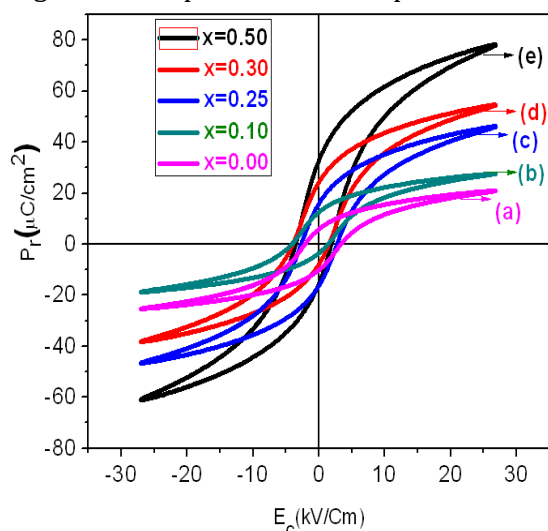


**Fig. 5 (a-e):** Ferroelectric hysteresis loop of the samples (a)  $PbTiO_3$ , (b)  $Pb_{0.9}La_{0.1}TiO_3$ , (c)  $Pb_{0.75}La_{0.25}TiO_3$ , (d)  $Pb_{0.70}La_{0.30}TiO_3$  and (e)  $Pb_{0.5}La_{0.5}TiO_3$  sintered at  $1100^\circ C$  for 4h.

**Table 3:** Observed values of  $P_r$ ,  $E_c$ ,  $P_s$  and  $P_r/P_s$  for  $Pb_{1-x}La_xTiO_3$ ,  $x = 0.0, 0.10, 0.25, 0.30$  and  $0.50$  at room temperature.

$(P_r/P_s)$	$P_s(\mu C/cm^2)$	$E_c(kV/cm)$	$P_r(\mu C/cm^2)$	x
0.881	18.30	4.18	16.14	0.00
0.780	25.34	3.43	19.77	0.10
0.471	43.01	3.18	20.29	0.25
0.520	52.84	1.87	27.51	0.30
0.469	75.81	1.81	35.56	0.50

#### 4. Conclusions

From Morphological study, it is observed that the grains are uniformly distributed throughout the surface. Grain size increases with increase of La concentration. A centrosymmetric cubic structure  $Pm\bar{3}m$  is expected since the material undergoes a phase transition to a paraelectric material. Ferroelectric to paraelectric transition has been observed in all the materials. Ferroelectric property diffuses with high La concentrations. The space charge polarization arises from the charge accumulation at grain boundaries and at electrode interfaces. A room temperature P-E loop reveals the ferroelectric ordering in the sample. remnant polarization ( $P_r$ ) was found to increase with La concentration from which one can predict that material gets ferroelectrically soften.

#### Acknowledgements

All the experimental works have been carried out using the facilities available at National Institute of Technology Rourkela, Orissa, India. The author is grateful to Dr Manoranjan Kar, Department of Physics, Indian Institute of Technology, Patna for his useful suggestions. Also, the author is thankful to Prof (Dr) S.S. Rath, vice chancellor Gangadhar Meher University, Sambalpur, for his valuable suggestions towards research publications.

#### References

- [1] K.K. Deb, *Ferroelectrics*, **82** (1998) 45.
- [2] P.M. Woodward, *Acta. Cryst.* **B53** (1997) 32-43.
- [3] N.Sahu, M.kar. and S. Panigrahi, *J. Arch. Phys. Res*, **1**(2010) (1)75-87.
- [4] N.Sahu, Manoranjan Kar, S.Panigrahi, *Int. J. phys.*, **3**(2010) (2)157-164.
- [5] N.Sahu, S.Panigrahi, Manoranjan Kar, *J.Adv.Powd.Tech.* **22**(2011)689-694.
- [6] N.Sahu, S. Panigrahi. *Bull. Mater. Sci.*, Vol. **34**, No. 7, 2011, pp. 1–6.
- [7] N.Sahu, S. Panigrahi, *Ceramics International* **38** (2012) 1085–1092.
- [8] N. Sahu, S. Panigrahi and M.Kar, *Ceramics International* **38** (2012) 1549–1556.
- [9] N.Sahu, and S.Panigrahi, *Bulletin of Material Science*, **36** (2013), page 699-708.
- [10] N.Sahu, *International journal in Physical and Applied Sciences IJPAS* (ISSN: 2394-5710) (2017) Scopus ID IJPAS: 6CBF50F057121EA7
- [11] K.Okazaki, K.Nagata. *Am Ceram Soc.* **52** (1973) 85.
- [12] M. Kuwabara, K.Goda, K. Oshima., *Phys. Rev. B* **42** (1990)10012.
- [13] Gurvinderjit Singh, V.S.Tiwari, *J.Appl.Phys.* **106** (2009)124104.
- [14] K. Wójcik, *Ferroelectrics*. **99** (1989) 5.
- [15] M. Kuwabara, K.Goda, K.Oshima., *Phys. Rev. B* **42** (1990)10012.
- [16] G. Shirane, R. Pepinsky, B. C. Frazer., *Phys. Rev.* **97** (1955)1179.
- [17] S. Bhattacharyya, A. Laha and S. B. Krupanidhi, *J. Appl. Phys.* **91** (2002) 4543.
- [18] D. K. Mahato, R. K. Choudhary, S. C. Srivastava, *J. Appl. Sci.* **6** (2006) 716.
- [19] G. Burns, F. Dacol, *Phys. Rev. B* **28** (1983) 2527.
- [20] J.J. Shyu, K.L. Mo, *Jpn. J. Appl. Phys.* **34** (1995) 5683.



- [21] E. A. Stern and Y. Yacoby, *J. Phys. Chem. Solids* **57** (1996)1449.
- [22] V. R. Mastelaro, P. P. Neves, A. Michalowicz, J. A. Eiras *AIP Conf. Proc.* **882** (2007) 496.
- [23] S. Singh, O. P. Thakur, C. Prakash, *Def. Sci. Jour.* **55** (2005) 349.
- [24] A. Mansingh, *Ferroelectrics.* **102** (1990) 69.
- [25] M.A.L. Nobre, S. Langfredi, *J. Phys. Chem.Solids* **62** (2001) 1999.
- [26] A.R. James, Chandra Prakash, G. Prasad, *J. Phys.D: Appl. Phys.* **39** (2006) 1635.
- [27] A. Mansingh, A. Dhar, *J. Phys. D: Appl. Phys.* **18** (1985) 2059.